

# Nitrogen-Vacancy Center as Open-Quantum-System Simulator

Chao Lei,<sup>1,2,3,\*</sup> Shijie Peng,<sup>1,\*</sup> Chenyong Ju,<sup>1,2</sup> Man-Hong Yung,<sup>4,†</sup> and Jiangfeng Du<sup>1,2,‡</sup>

<sup>1</sup>Hefei National Laboratory for Physics Sciences at Microscale and Department of Modern Physics,  
University of Science and Technology of China, Hefei, 230026, China

<sup>2</sup>Synergetic Innovation Center of Quantum Information and Quantum Physics,  
University of Science and Technology of China, Hefei, Anhui 230026, People's Republic of China

<sup>3</sup>Department of Physics, The University of Texas at Austin, Austin, Texas 78712, USA

<sup>4</sup>Department of Physics, South University of Science and Technology of China,  
Shenzhen, Guangdong, 518055, People's Republic of China

Quantum mechanical systems lose coherence through interactions with external environments—a process known as decoherence. Although decoherence is detrimental for most of the tasks in quantum information processing, a substantial degree of decoherence is crucial for boosting the efficiency of quantum processes, for example, in quantum biology. The key to the success in simulating those open quantum systems is therefore the ability of controlling decoherence, instead of eliminating it. Here we focus on the problem of simulating quantum open systems with Nitrogen-Vacancy centers, which has become an increasingly important platform for quantum information processing tasks. Essentially, we developed a new set of steering pulse sequences for controlling various coherence times of Nitrogen-Vacancy centers; our method is based on a hybrid approach that exploits ingredients in both digital and analog quantum simulations to dynamically couple or decouple the system with the physical environment. Our numerical simulations, based on experimentally-feasible parameters, indicate that decoherence of Nitrogen-Vacancy centers can be controlled externally to a very large extent.

PACS numbers: 03.67.Ac, 03.65.Sq, 03.65.Yz,

**Introduction—** A quantum simulator [1–5] is potentially a powerful tool for solving many-body problems that are not tractable by classical methods. Generally, there are two types of quantum simulators. The first type, called digital quantum simulator [2, 6–10], makes use of a general-purpose quantum computer, where quantum states are encoded with qubits and the dynamical evolution is programmed in a quantum circuit. The other kind of quantum simulators are called analog quantum simulators [11–15], where the Hamiltonian of the simulated quantum system is directly engineered in a dedicated quantum device, for example, trapped ions [13, 16] and optical lattices [17].

The main challenge of constructing a practical quantum simulator is to reduce the influence of environmental decoherence, a universal problem for all tasks in quantum information processing including quantum communication [18]. In practice, a quantum simulator is necessarily an *open quantum system*, where the underlying system-environment interaction [19] plays the main role in determining the performance of a quantum simulator. Furthermore, it is important to understand how a quantum simulator can simulate open quantum systems [19], which are of fundamental importance for understanding many physical phenomena in, for example, quantum optics [20], quantum measurement [21], and biological systems [22].

In the literature, digital approaches of open-system quantum simulation [23–26] have been theoretically studied and experimentally demonstrated. Similarly, analog quantum simulators of open quantum system has been theoretically pro-

posed [27] and experimentally investigated [28]. An important approach to tackle the decoherence problem, called dynamical decoupling [29–35], have been developed to significantly eliminate the system-environment interactions [36], through a sequence of external pulses applied to the system. Experimental implementations of dynamical decoupling indicate that such approach is widely applicable to various experimental platforms [37–44]. Moreover, an extension of dynamical decoupling is possible for universal quantum computation [45, 46] and other applications [47, 48].

Here we study the possibility of simulating *open* quantum systems through an extension of the idea of dynamical decoupling. More precisely, we developed a new set of decoupling pulse sequences that can control the coherence times of the off-diagonal matrix elements of the system density matrix.

The pulse sequences of interest in this work are different from those in dynamical decoupling [29–31], which primary goal is to *decouple* the system from the influence of the environment. In other words, the goal of dynamical decoupling was to maintain the purity of the quantum system. Here we aims to *control* the decoherence by exploiting the existing environment, so that we can simulate the dynamics of an open quantum system without the need to maintain the purity of the system. Consequently, we can avoid the need of including extra ancilla qubits as in other digital approaches of simulating open quantum systems.

**Full system controllability—** A NV center can be viewed as a 3-dimensional qudit with a Hamiltonian  $H_{NV}$  of the following form [39, 49, 50]:

$$H_{NV} = DS_z^2 + \gamma B_z S_z, \quad (1)$$

where  $S_z$  is the 3-dimensional spin operator for the spin-1 particle  $\{m = 1, 0, -1\}$ ,  $D$  is the zero-field splitting,  $\gamma = g\mu_B$  is the gyromagnetic ratio with  $\mu_B$  the Bohr mag-

\* These two authors contributed equally

† Corresponding author: yung@sustc.edu.cn

‡ Corresponding author: djf@ustc.edu.cn

netism,  $g$  the  $g$ -factor of electron, and  $B_z$  is the static magnetic field applied along  $z$  direction ([111] axis). Before we demonstrate how to control decoherence, we first show how to simulate a general  $d$ -dimensional system with a NV center. For a chosen basis  $\{|m\rangle\}$ , the Hamiltonian  $H_S$  of a general  $d$ -dimensional system can be expressed as:  $H_S = \sum_{m=0}^{d-1} \varepsilon_m |m\rangle \langle m| + \sum_{m < n}^{d-1} (J_{mn} |m\rangle \langle n| + J_{mn} |n\rangle \langle m|)$ , where  $\varepsilon_m = \langle m| H_S |m\rangle$  is the energy of the  $m$ -th state  $|m\rangle$ , and  $J_{mn} = \langle m| H_S |n\rangle$  is the coupling between the  $m$  and  $n$ -th state.

For any given Hamiltonian  $\hat{H}$  and quantum state  $|\Psi\rangle$ , and a unitary operator  $\hat{U} = e^{-i\hat{A}t}$  associated with a self-adjoint operator  $\hat{A}$ , the corresponding quantum state in the rotating frame is given by,  $|\Psi_{\text{rot}}\rangle \equiv \hat{U}^\dagger |\Psi\rangle$ . We can obtain an effective Hamiltonian  $H_{\text{rot}}$  in the rotational frame as follows:  $H_{\text{rot}} = \hat{U}^\dagger \hat{H} \hat{U} - \hat{A}$ . In our case, we include two sets of microwave pulses to a NV center. In the laboratory frame, the Hamiltonian in Eq. (1) becomes:

$$H_{NV}^{mw} = H_{NV} + \gamma B_1 S_x \cos \omega_1 t + \gamma B_2 S_x \cos \omega_2 t, \quad (2)$$

where  $H_{NV}$  is the Hamiltonian shown as in Eq. (1),  $S_x$  is a  $3 \times 3$  spin operator,  $B_1$  and  $B_2$  are the applied magnetic field along the  $\hat{x}$  axis, and  $\omega_1$  and  $\omega_2$  are the frequencies of the applied microwave.

The target Hamiltonian  $H_S$  can be obtained by choosing a rotational frame reference where  $\hat{A} = \omega_1 |1\rangle \langle 1| + \omega_2 |1\rangle \langle -1|$ , which gives the following:  $\varepsilon_1 = D + \gamma B_z - \omega_1$ ,  $\varepsilon_2 = 0$ ,  $\varepsilon_3 = D + \gamma B_z - \omega_2$ ,  $J_{12} = \gamma B_1 / 2\sqrt{2}$ , and  $J_{23} = \gamma B_2 / 2\sqrt{2}$ . When the coupling parameters are taken to be some real values, the  $3 \times 3$  version of the Hamiltonian in Eq. (1) contains 4 free parameters (apart from an overall shift of the total energy).

**Noises in Nitrogen-Vacancy (N-V) centers—** For a general open quantum system, the Hamiltonian  $H$  can be divided into three parts:  $H = H_S + H_{SB} + H_B$ , where  $H_S$  is the Hamiltonian of quantum system,  $H_{SB}$  is the Hamiltonian of the system-environment interaction, and  $H_B$  is the Hamiltonian of environment (bath). Normally, a NV center is subject to a local environment dominated by the surrounding nuclear spins of  $^{13}\text{C}$ 's and electron spins of P1 centers, which effectively produce a random magnetic field  $b(t)$  to the NV center [39, 49], i.e.,  $H_{SB} = b(t) S_z = b(t) (|1\rangle \langle 1| - |1\rangle \langle -1|)$ .

For the cases where the environment is dominated by the nuclear spins, the random fluctuation of the magnetic field can be regarded as stationary, i.e.,  $b(t) = b$ , and is usually approximated as Markovian and Gaussian [49], i.e., with a probability distribution  $\text{Pr}(b) = e^{-b^2/2\sigma_b^2} / \sqrt{2\pi}\sigma_b$ , where  $\sigma_b$  is the variance of the random magnetic field from the spin bath. For the cases where the noise come from electron spins instead, the random process of  $b(t)$  can be approximated by the Ornstein-Uhlenbeck process [39], with a correlation function  $C(t)$  given by the following,  $C(t) = \langle b(0)b(t) \rangle = l^2 \exp(-R|t|)$ , where  $l$  describes the characteristic strength of the coupling of the NV center to the bath, and  $R = 1/\tau_c$  is the transition rate, with  $\tau_c$  being the correlation time of the spin bath [39].

**Strengthening decoherence—** We note that the evolution operator  $e^{-iHt}$  of the total system can be divided by many small time slices,  $\Delta t \equiv t/n$ ,  $e^{-iHt} = \lim_{n \rightarrow \infty} (e^{-iH_S \Delta t} e^{-iH_{SB} \Delta t} e^{-iH_B \Delta t})^n$ . One way to strengthen decoherence, assisted by the environment, can be achieved as follows: first, turn off the system Hamiltonian momentarily (setting  $H_S = 0$ ), for a time period,  $\lambda \Delta t$ , where  $\lambda > 0$ , i.e.,  $e^{-i(H_{SB} + H_B) \lambda \Delta t}$ . Then we allow the total system to evolve freely for a time period of  $\Delta t$ . The pattern is then repeated for  $n$  times, i.e.,  $(e^{-i(H_S + H_{SB} + H_B) \Delta t} e^{-i(H_{SB} + H_B) \lambda \Delta t})^n$ . Therefore, in the large- $n$  limit, we obtain an effective Hamiltonian as follows,

$$H_{\text{eff}} = H_S + (1 + \lambda)(H_{SB} + H_B), \quad (3)$$

which contains an interaction term  $H_{SB}$  amplified by a factor of  $(1 + \lambda)$ . The side product is that the energies of the environment is also amplified. However, for the spin environments of NV centers, the effect can be ignored.

**Controlling noises from nuclear and electron spin baths—** In the following we consider combining Trotter expansion with decoupling pulses to control the decoherence in NV centers. For NV centers in ultra-pure diamonds, the dominant decoherence source comes from the surrounding  $^{13}\text{C}$  spin bath [49], which is random but stationary within the time-scale of system dynamics. Consequently, for a qubit initialized in a pure state,  $|\psi_0\rangle = \alpha|0\rangle + \beta|1\rangle$ , and  $H_S = 0$ , the off-diagonal matrix element (or coherence),  $\rho_{12} = \alpha\beta^* \int \text{Pr}(b) e^{-i2b(1+\lambda)t} db$ , decays as follows:  $\rho_{12} = \alpha\beta^* e^{-2\sigma_b^2(1+\lambda)^2 t^2}$ , which implies that the effective decoherence time  $T_2$ , can be controlled by the parameter  $\lambda$ ,

$$T_2(\lambda) = 1/\sqrt{2}\sigma_b(1 + \lambda). \quad (4)$$

From Fig.1(a), it is clear that tuning the parameter  $\lambda$  can strengthen the decoherence, i.e., we can destroy the coherence via increasing the value of  $\lambda$ . The coherence time can be extract from above and shown in Fig. 1(b).

In diamonds with nitrogen impurities, such as Type I, the electron spins also contribute to the decoherence of the system, which means that both nuclear and electron noise should be included. We investigate the decoherence of a two-level system numerically with experimental parameters of NV center. The simulated results are shown in Fig.1 (c) and (d), in which one microwave is applied. The parameters are as follow: The static magnetic field is  $B_z = 100$  Gauss, the zero-field splitting is  $D = 2.87\text{GHz}$ , the frequency of applied microwave is a little away from the resonance frequency (which is 3.15 GHz) of NV center at the given static magnetic field with a detuning  $1.9 \times 10^6/(1+\lambda)$  Hz and with a amplitude of 1.717 Gauss,  $\lambda$  is varied from zero (i.e. the  $T_2^*$ ) to 3. the coherence time vs  $\lambda$  is shown in Fig.1 (d), it shows that the coherence time of NV center decrease when  $\lambda$  increases, which shows a effective control of decoherence caused by system-environment interaction.

**Weakening decoherence—** Let us consider a two-level system and a swap gate defined by:  $u_{12} \equiv \sigma_x = \begin{pmatrix} 0 & 1 \\ 1 & 0 \end{pmatrix}$ . During the decoupling part of Trotter decomposition, we include the following evolution:

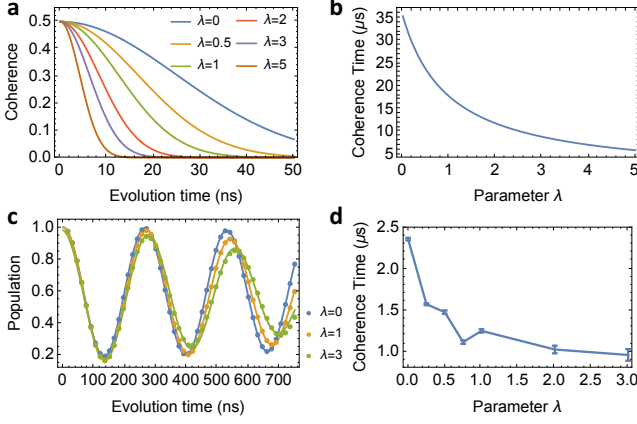


FIG. 1. (Color online) (a) Coherence vs evolution time, the variance of the random magnetic field is set to be 0.2 Gauss. (b) Coherence time vs  $\lambda$ . (c) Evolution of population with time, the dots are simulated points and the curves are fitted one. (d) Coherence time got from the fitting curve in (c) vs  $\lambda$  from 0 to 3, here the values of  $\lambda$  in the calculation are 0, 0.25, 0.5, 0.75, 1, 2, 3.

$\sigma_x e^{-iH_{SB}t_2} \sigma_x e^{-iH_{SB}t_1} = e^{-iH_{SB}(t_1-t_2)}$ , where we set  $t_1 = (\lambda - \mu)\Delta t$  and  $t_2 = \mu\Delta t$ . The overall evolution becomes  $(e^{-i(H_S+H_{SB})\Delta t} e^{-iH_{SB}(\lambda-2\mu)\Delta t})^n$ , which implies the following effective Hamiltonian:

$$H_{\text{eff}} = H_S + (1 + \lambda - 2\mu)H_{SB} \quad (5)$$

Suppose  $H_S = 0$ , the coherence vs evolution time under Eq. (5) becomes:  $\rho_{12} = \alpha\beta^* e^{-2\sigma_b^2(1+\lambda-2\mu)^2 t^2}$ . This is shown in Fig. 2(a) and the coherence time is:

$$T_2^{\text{dd}} = 1/\sqrt{2}\sigma_b(1 + \lambda - 2\mu), \quad (6)$$

which is shown in Fig. 2(b). Here we set the distance between two swap gate as  $\mu\Delta t = \tau\lambda\Delta t/2$ . When  $\tau = 0$ , it is equal to the case with no decoupling pulse, but when  $\tau = 1$ , the distance between the two swap gate is half of the  $\lambda\Delta t$ , which is the same as the CPMG pulse [51, 52].

In the presence of electron spin noise, the coherence factor of a two-level system subject to dynamical decoupling is given [53] by,  $W(t) = |\langle \exp(-i \int_0^t b(t') f(t; t') dt') \rangle| = e^{\chi(t)}$ , where  $b(t)$  is the random noise, the function  $f(t; t')$  depends on the pulse sequence as,  $f(t; t') = \sum_{k=0}^n (-1)^k \theta(t_{k+1} - t') \theta(t' - t_k)$ , with  $\theta(t')$  the Heaviside step function,  $t_0 = 0$  and  $t_{n+1} = t$  is the total evolution time.

Furthermore, the spectral density of the noise  $C(\omega)$  is given [39] by,  $C(\omega) = l^2 \frac{2R}{R^2 + \omega^2}$ , which implies that  $\chi(t) = \int_0^\infty \frac{d\omega}{2\pi} C(\omega) |\tilde{f}(t, \omega)|^2$ , where  $\tilde{f}(t, \omega) = \int_{-\infty}^\infty e^{i\omega t} f(t; t') dt$ . For our case, the square of Fourier transform of  $f(t; t')$  is found to be,  $|\tilde{f}(t, \omega)|^2 = \frac{1}{\omega^2} \frac{1 - \cos \omega t}{1 - \cos \omega \delta} (6 + 2 \cos \omega \delta - 4 \cos \omega \delta_1 - 4 \cos \omega \delta_2)$ , where  $\delta = \lambda\Delta t$ ,  $\delta_1 = (\lambda - \mu)\Delta t$  and  $\delta_2 = \mu\Delta t$ . The values of  $|\tilde{f}(t, \omega)|^2$  are shown in Fig. 2(c) with different values of  $\tau$ , which is defined in the following relation,  $\mu\Delta t = \tau\lambda\Delta t/2$ . We obtained the coherence factor shown as in Fig. 2(d), after applying a large cut-off frequency.

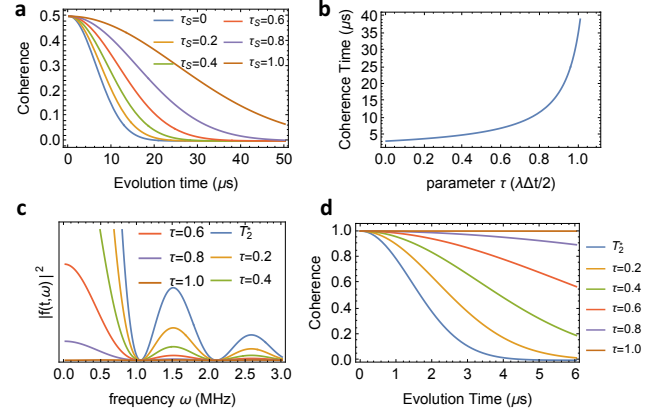


FIG. 2. (Color online) (a) Coherence vs evolution time with different distance between two swap gate, the variance of the random magnetic field is set to be 0.2 Gauss. (b) Coherence time vs  $\tau$ , which is defined in  $\mu\Delta t = \tau\lambda\Delta t/2$ . (c) is the values of  $|\tilde{f}(t, \omega)|^2$  which represent the noise spectrum. (d) The coherence vs time with different  $\tau$ .

It is obviously that when  $\tau$  becomes larger, the coherence time becomes longer.

**Fine-tuning decoherence for qudit**—For a general multi-level systems, i.e., qudit, we have an extra tool to fine-tuning the decoherence for different off-diagonal elements in the density matrix. Here we consider only the stationary noise from nuclear spin in three-level system. Let us consider applying the dynamical decoupling pulses,  $u_{12} = |1\rangle\langle 0| + |0\rangle\langle 1| + |-1\rangle\langle -1|$ , are applied on only one channel, between  $|m=1\rangle$  and  $|m=0\rangle$ , then the relevant part in evolution operator becomes:  $u_{12} e^{-iH_{SB}t_2} u_{12} e^{-iH_{SB}t_1} \equiv e^{-ib(t)L(t_1, t_2)}$ , where  $L(t_1, t_2) = |1\rangle\langle 1| t_1 + |0\rangle\langle 0| t_2 - |-1\rangle\langle -1| (t_1 + t_2)$ . Therefore, when we choose  $t_1 < t_2$ , we effectively make state  $|1\rangle$  experience less dephasing than state  $|0\rangle$ , and vice versa.

As an example, we again set:  $t_1 = (\lambda - \mu)\Delta t$  and  $t_2 = \mu\Delta t$ , which gives  $t_1 + t_2 = \lambda\Delta t$ . For any given initial state,  $\psi_0 = \alpha|1\rangle + \beta|0\rangle + \gamma|-1\rangle$ , if we set  $H_S = 0$ , then the off diagonal elements of the associated density matrix decays as follows:  $\rho_{12} = \alpha\beta^* e^{-\sigma_b^2(1+\lambda-2\mu)^2 t^2/2}$ ,  $\rho_{13} = \alpha\gamma^* e^{-\sigma_b^2(2+2\lambda-\mu)^2 t^2/2}$ , and  $\rho_{23} = \beta\gamma^* e^{-\sigma_b^2(1+\lambda+\mu)^2 t^2/2}$ . In other words, the coherence times of the off-diagonal elements are given by  $T_2^{12} = \sqrt{2}/\sigma_b(1 + \lambda - 2\mu)$ ,  $T_2^{13} = \sqrt{2}/\sigma_b(2 + 2\lambda - \mu)$ , and  $T_2^{23} = \sqrt{2}/\sigma_b(1 + \lambda + \mu)$ .

The dependence of the coherence times with the parameter  $\mu$  is shown in Fig. 3(a). We see that the coherence time  $T_2^{12}$  is more sensitive to the change of  $\mu$ , compared with the other coherence times.

Furthermore, additional dynamical decoupling pulses, e.g.,  $u_{23} = |1\rangle\langle 1| + |-1\rangle\langle 0| + |0\rangle\langle -1|$ , can be applied, between  $|m=-1\rangle \leftrightarrow |m=0\rangle$  and  $|m=0\rangle \leftrightarrow |m=1\rangle$ , then we have (let  $\mu_2 > \mu_1$ ):  $u_{23} u_{12} e^{-iH_{SB}t_3} u_{12} e^{-iH_{SB}t_2} u_{23} e^{-iH_{SB}t_1} \equiv e^{-ib(t)L(t_1, t_2, t_3)}$ , where  $L(t_1, t_2, t_3) = |1\rangle\langle 1| (t_1 + t_2) - |0\rangle\langle 0| (t_2 + t_3) - |-1\rangle\langle -1| (t_1 - t_3)$ . Suppose we set  $t_1 = (\lambda - \mu_2)\Delta t$ ,  $t_2 = (\mu_2 - \mu_1)\Delta t$  and

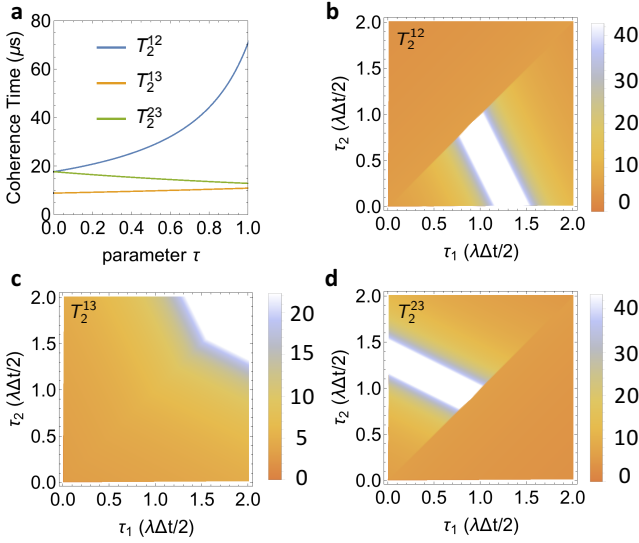


FIG. 3. (Color online) (a) The coherence time vs  $\tau$  (which is defined in  $\mu\Delta t = \tau\lambda\Delta t/2$ ), as  $\tau$  increases, the coherence time  $T_2^{12}$  increases and the other two coherence time remains almost the same, decrease or increase slightly. (b)-(d) show the coherence time between the three levels, with (b) is the  $T_2^{12}$ , (c) the  $T_2^{13}$  and (d)  $T_2^{23}$ , in which  $\tau_1$  and  $\tau_2$  are defined in  $\mu_{1(2)}\Delta t = \tau_{1(2)}\lambda\Delta t/2$ , the blue region means the coherence time is small and the red ones is the case the coherence time increases sharply.

$t_3 = \mu_1\Delta t$  (shown in Fig. 3a) with  $0 \leq \mu_1 \leq \lambda$  and  $\mu_1 \leq \mu_2 \leq \lambda$ . It gives  $t_1 + t_2 + t_3 = \lambda\Delta t$ . Consequently, for any initial state,  $\psi_0 = \alpha|1\rangle + \beta|0\rangle + \gamma|-1\rangle$ , the time-dependent off-diagonal elements of the density matrix are given by:  $\rho_{12}(t) = \alpha\beta^* e^{-\frac{1}{2}\sigma_b^2(1+\lambda-(\mu_1-\mu_2))^2 t^2}$ , and similarly for  $\rho_{13}(t) = \alpha\gamma^* e^{-\frac{1}{2}\sigma_b^2(2+2\lambda-(2\mu_1+\mu_2))^2 t^2}$  and  $\rho_{23}(t) = \beta\gamma^* e^{-\frac{1}{2}\sigma_b^2(1+\lambda-(\mu_1+2\mu_2))^2 t^2}$ , which means that the coherence times of the off-diagonal elements are given by,  $T_2^{12} = \sqrt{2}/\sigma_b(1+\lambda-(\mu_1-\mu_2))$  for  $\rho_{12}(t)$ ,  $T_2^{13} = \sqrt{2}/\sigma_b(2+2\lambda-(2\mu_1+\mu_2))$  for  $\rho_{13}(t)$ , and

$$T_2^{23} = \sqrt{2}/\sigma_b(1+\lambda-(\mu_1+2\mu_2)) \text{ for } \rho_{23}(t).$$

The coherence times with parameters  $\mu_{1(2)}$  are shown in Fig. 3(b)-(d) (in which the case of  $\tau_2 \leq \tau_1 \leq 2$  is also included, where  $\tau_1$  and  $\tau_2$  are defined in  $\mu_{1(2)}\Delta t = \tau_{1(2)}\lambda\Delta t/2$ ). In the plots, the blue region means the coherence time is small and the red ones is the case the coherence time increases sharply. It shows that the coherence between different levels can be tuned though changing the insert time of the two decoupling time, which is similar with the case of only one channel is applied with decoupling pulse. The decoupling pulses are applied on both channels; the coherence time  $T_2^{13}$  increases when  $\mu_1$  and  $\mu_2$  are close to  $\lambda$  (shown in Fig. 3(c)), while the other two coherence time remains essentially the same as the one before applying the decoupling pulses.

Finally, further generalization of our method to  $d$ -dimensional ( $d \geq 4$ ) systems is possible. Following the previous results, the decoherence of different off-diagonal elements can be controlled by the following sequence:  $\prod_{i<j} u_{ij} \prod_{i<j} [e^{-iH_{SB}t_{ij}} u_{ij}] e^{-iH_{SB}t_0} e^{-i(H_S+H_{SB})\Delta t}$ , where  $t_{ij}$ 's are the adjustable waiting time before the swap gate between  $i$  and  $j$  level is applied after the next swap gate  $u_{ij} = I + |i\rangle\langle j| + |j\rangle\langle i| - |i\rangle\langle i| - |j\rangle\langle j|$ , where  $t_0$  is included as the waiting time before the first swap gate applied.

**Conclusion—** In conclusions, in this work, we have presented a new method that can engineer the environment induced decoherence by combining the Trotter decomposition and decoupling pulses. The scheme exploits the intrinsic decoherence from the environment, and contains the benefits of the universality of digital quantum simulation and also the efficiency of analog quantum simulation. This hybrid simulation method is numerically tested for NV centers with two and three energy levels. Our results indicate that such a scheme is experimentally feasible.

**Acknowledgements** This work was supported by the National Key Basic Research Program of China (Grant No. 2013CB921800), the National Natural Science Foundation of China (Grant Nos. 11227901 and 11405093), and the Strategic Priority Research Program (B) of the CAS (Grant No. XDB01030400).

- 
- [1] R. P. Feynman, *Int. J. Theor. Phys.*, **21** (1982).
  - [2] S. Lloyd, *Science*, **273** (1996).
  - [3] I. Buluta and F. Nori, *Science*, **326**, 108 (2009).
  - [4] I. Kassal, J. D. Whitfield, A. Perdomo-Ortiz, M.-H. Yung, and A. Aspuru-Guzik, *Annu. Rev. Phys. Chem.*, **62**, 185 (2011), ISSN 0066-426X.
  - [5] M.-H. Yung, J. D. Whitfield, S. Boixo, D. G. Tempel, and A. Aspuru-Guzik, in *Adv. Chem. Phys.*, Vol. 154, edited by S. Kais (John Wiley & Sons, Inc., New Jersey, 2014) pp. 67–106, ISBN 9781118742631.
  - [6] B. Lanyon, C. Hempel, D. Nigg, M. Müller, R. Gerritsma, F. Zähringer, P. Schindler, J. Barreiro, M. Rambach, G. Kirchmair, *et al.*, *Science*, **334**, 57 (2011).
  - [7] J. Zhang, M.-H. Yung, R. Laflamme, A. Aspuru-Guzik, and J. Baugh, *Nat. Commun.*, **3**, 880 (2012), ISSN 2041-1723.
  - [8] M.-H. Yung and A. Aspuru-Guzik, *Proc. Natl. Acad. Sci.*, **109**, 754 (2012), ISSN 0027-8424.
  - [9] Z. Li, M.-H. Yung, H. Chen, D. Lu, J. D. Whitfield, X. Peng, A. Aspuru-Guzik, and J. Du, *Sci. Rep.*, **1**, 88 (2011), ISSN 2045-2322.
  - [10] M.-H. Yung, J. Casanova, A. Mezzacapo, J. McClean, L. Lamata, A. Aspuru-Guzik, and E. Solano, *Sci. Rep.*, **4**, 3589 (2014), ISSN 2045-2322.
  - [11] S. Somaroo, C. H. Tseng, T. F. Havel, R. Laflamme, and D. G. Cory, *Phys. Rev. Lett.*, **82**, 5381 (1999).
  - [12] L. Lamata, J. León, T. Schätz, and E. Solano, *Phys. Rev. Lett.*, **98**, 253005 (2007).
  - [13] R. Gerritsma, G. Kirchmair, F. Zähringer, E. Solano, R. Blatt, and C. F. Roos, *Nature*, **463**, 68 (2010).
  - [14] M.-H. Yung, X. Gao, and J. Huh, [arXiv:1608.00383](https://arxiv.org/abs/1608.00383).
  - [15] J. Huh and M.-H. Yung, [arXiv:1608.03731](https://arxiv.org/abs/1608.03731).
  - [16] Y. Shen, X. Zhang, S. Zhang, J.-N. Zhang, M.-H. Yung, and



- K. Kim, [arXiv:1506.00443](https://arxiv.org/abs/1506.00443).
- [17] M. Greiner and S. Folling, *Nature*, **453**, 736 (2008).
  - [18] J.-S. Xu, M.-H. Yung, X.-Y. Xu, J.-S. Tang, C.-F. Li, and G.-C. Guo, *Sci. Adv.*, **2**, e1500672 (2016), ISSN 2375-2548.
  - [19] H.-P. Breuer and F. Petruccione, *The theory of open quantum systems* (Oxford university press, Oxford, 2002).
  - [20] M. O. Scully and M. S. Zubairy, *Quantum optics* (Cambridge university press, New York, 1997).
  - [21] M. Schlosshauer, *Rev. Mod. Phys.*, **76**, 1267 (2005).
  - [22] D. Suess, A. Eisfeld, and W. Strunz, *Phys. Rev. Lett.*, **113**, 150403 (2014).
  - [23] D. Bacon, A. M. Childs, I. L. Chuang, J. Kempe, D. W. Leung, and X. Zhou, *Phys. Rev. A*, **64**, 062302 (2001).
  - [24] M.-H. Yung, D. Nagaj, J. D. Whitfield, and A. Aspuru-Guzik, *Phys. Rev. A*, **82**, 060302 (2010), ISSN 1050-2947.
  - [25] J.-S. Xu, M.-H. Yung, X.-Y. Xu, S. Boixo, Z.-W. Zhou, C.-F. Li, A. Aspuru-Guzik, and G.-C. Guo, *Nat. Photonics*, **8**, 113 (2014), ISSN 1749-4885.
  - [26] R. Sweke, I. Sinayskiy, and F. Petruccione, *Phys. Rev. A*, **90**, 022331 (2014).
  - [27] S. Mostame, P. Rebentrost, A. Eisfeld, A. J. Kerman, D. I. Tsomokos, and A. Aspuru-Guzik, *New J. Phys.*, **14**, 105013 (2012).
  - [28] M. Haeberlein, F. Deppe, A. Kurcz, J. Goetz, A. Baust, P. Eder, K. Fedorov, M. Fischer, E. P. Menzel, M. J. Schwarz, *et al.*, [arXiv:1506.09114](https://arxiv.org/abs/1506.09114) (2015).
  - [29] L. Viola, E. Knill, and S. Lloyd, *Phys. Rev. Lett.*, **82**, 2417 (1999).
  - [30] K. Khodjasteh and D. Lidar, *Phys. Rev. Lett.*, **95**, 180501 (2005).
  - [31] G. S. Uhrig, *Phys. Rev. Lett.*, **98**, 100504 (2007).
  - [32] W. Yang and R.-B. Liu, *Phys. Rev. Lett.*, **101**, 180403 (2008).
  - [33] G. Gordon, G. Kurizki, and D. A. Lidar, *Phys. Rev. Lett.*, **101**, 010403 (2008).
  - [34] G. S. Uhrig, *Phys. Rev. Lett.*, **102**, 120502 (2009).
  - [35] J. R. West, B. H. Fong, and D. A. Lidar, *Phys. Rev. Lett.*, **104**, 130501 (2010).
  - [36] H.-P. Breuer, E.-M. Laine, J. Piilo, and B. Vacchini, *Rev. Mod. Phys.*, **88**, 021002 (2016).
  - [37] M. J. Biercuk, H. Uys, A. P. VanDevender, N. Shiga, W. M. Itano, and J. J. Bollinger, *Nature*, **458**, 996 (2009).
  - [38] J. Du, X. Rong, N. Zhao, Y. Wang, J. Yang, and R. B. Liu, *Nature*, **461**, 1265 (2009).
  - [39] G. De Lange, Z. Wang, D. Riste, V. Dobrovitski, and R. Hanson, *Science*, **330**, 60 (2010).
  - [40] Y. Sagi, I. Almog, and N. Davidson, *Phys. Rev. Lett.*, **105**, 053201 (2010).
  - [41] D. V. Averin, K. Xu, Y. P. Zhong, C. Song, H. Wang, and S. Han, *Phys. Rev. Lett.*, **116**, 010501 (2016).
  - [42] H. Bluhm, S. Foletti, I. Neder, M. Rudner, D. Mahalu, V. Umansky, and A. Yacoby, *Nat Phys*, **7**, 109 (2011).
  - [43] J. Medford, L. Cywiński, C. Barthel, C. M. Marcus, M. P. Hanson, and A. C. Gossard, *Phys. Rev. Lett.*, **108**, 086802 (2012).
  - [44] C. A. Ryan, J. S. Hodges, and D. G. Cory, *Phys. Rev. Lett.*, **105**, 200402 (2010).
  - [45] J. R. West, D. A. Lidar, B. H. Fong, and M. F. Gyure, *Phys. Rev. Lett.*, **105**, 230503 (2010).
  - [46] A. M. Souza, G. A. Álvarez, and D. Suter, *Phys. Rev. Lett.*, **106**, 240501 (2011).
  - [47] K. Khodjasteh, D. A. Lidar, and L. Viola, *Phys. Rev. Lett.*, **104**, 090501 (2010).
  - [48] G. Wolfowicz, M. Urdampilleta, M. L. W. Thewalt, H. Riemann, N. V. Abrosimov, P. Becker, H.-J. Pohl, and J. J. L. Morton, *Phys. Rev. Lett.*, **113**, 157601 (2014).
  - [49] R. Hanson, V. Dobrovitski, A. Feiguin, O. Gywat, and D. Awschalom, *Science*, **320**, 352 (2008).
  - [50] R. Hanson, O. Gywat, and D. D. Awschalom, *Phys. Rev. B*, **74**, 161203 (2006).
  - [51] H. Y. Carr and E. M. Purcell, *Phys. Rev.*, **94**, 630 (1954).
  - [52] S. Meiboom and D. Gill, *Rev. Sci. Instrum.*, **29**, 688 (1958).
  - [53] Ł. Cywiński, R. M. Lutchyn, C. P. Nave, and S. D. Sarma, *Phys. Rev. B*, **77**, 174509 (2008).